Journal of Solid State Chemistry 183 (2010) 2110–2115

Contents lists available at ScienceDirect

Journal of Solid State Chemistry

journal homepage: www.elsevier.com/locate/jssc

$Y_2O_3:Eu^{3+}$ (5 mol%) with Ag nanoparticles prepared by citrate precursor

J.L. Ferrari [a,*], M.A. Cebim [a], A.M. Pires [b], M.A. Couto dos Santos [c], M.R. Davolos [a]

[a] Instituto de Química, UNESP Univ. Estadual Paulista, 14800-970, Araraquara–São Paulo, Brazil
[b] Depto. de Física, Química e Biologia, Faculdade de Ciências e Tecnologia, UNESP Univ Estadual Paulista, P.O. Box 467, 19060-900, Presidente Prudente, São Paulo, Brazil
[c] Departamento de Física/UFS, 49100-000 São Cristóvão/SE/Brazil

ARTICLE INFO

Article history:
Received 11 February 2010
Received in revised form
5 June 2010
Accepted 12 July 2010
Available online 15 July 2010

Keywords:
Yttrium oxide
Europium ion
Ag nanoparticles
Luminescence spectroscopy

ABSTRACT

$Y_2O_3:Eu^{3+}$ (5 mol% Eu^{3+}) and $Y_2O_3:Eu^{3+}$ (5 mol% Eu^{3+}) containing 1 mol% of Ag nanoparticles were prepared by heat treatment of a viscous resin obtained via citrate precursor. TEM and EDS analyses showed that $Y_2O_3:Eu^{3+}$ (5 mol% Eu^{3+}) is formed by nanoparticles with an average size of 12 nm, which increases to 30 nm when Ag is present because the effect of metal induced crystallization occurs. Ag nanoparticles with a size of 9 nm dispersed in $Y_2O_3:Eu^{3+}$ (5 mol% Eu^{3+}) were obtained and the surface plasmon effect on Ag nanoparticles was observed. The emission around 612 nm assigned to the Eu^{3+} ($^5D_0 \rightarrow {}^7F_2$) transition enhanced when the Ag nanoparticles were present in the $Y_2O_3:Eu^{3+}$ luminescent material.

1. Introduction

Europium-activated Y_2O_3 ($Y_2O_3:Eu^{3+}$) has attracted much attention as a red-emitting phosphor for commercial use in fluorescent lighting and screen due to its high luminescence emission around 612 nm. Because of the fast development of nanotechnology, the optical properties of nanocrystalline $Y_2O_3:Eu^{3+}$ have also been extensively investigated for its potential application in high resolution imaging for flat plasma displays and in fundamental research [1,2]. Therefore, many researchers have already performed investigations related to this nanophosphor, such as the study of the influence of particle size on the intense luminescence of nanocrystalline $Y_2O_3:Eu^{3+}$ [3–12].

In order to achieve improved luminescent properties of $Y_2O_3:Eu^{3+}$ [13], the precursors as well as the synthetic route are very important factors. In the literature, many papers have reported different routes used to prepare this material, for example EDTA complex sol–gel process [14], combustion synthesis [15,16], flame spray pyrolysis [17,18], low temperature hydrothermal route [19], firing precursors prepared by urea thermal decomposition [20], microemulsion microwave heating [21], reverse micelles [22], sol–gel process [23–25], homogeneous precipitation technique [26], Au nanoparticles dispersed in $Y_2O_3:Eu^{3+}$ films [27], and the citrate method [30]. The use of citrate precursors has been reported as a way to achieve materials with excellent features [31]. The use of citric acid (alpha-hydroxycarboxilic acid) contributes to form the stable chelates through carboxylic groups with different metals and provides precursors with a high level of homogeneity.

Besides, nanostructured metallic surfaces appear as an alternative to enhance the luminescence of $Y_2O_3:Eu^{3+}$. Liu et al. [32] have assigned the luminescence enhancement of $Y_2O_3:Eu^{3+}$ to an energy transfer from Ag to this material. Metallic nanostructures have caused a drastic increase in the intensity of Raman scattering or luminescence ions in close proximity with the metallic surface [33]. $Y_2O_3:Eu^{3+}$ containing Au nanoparticles has also been reported with an increase of luminescence compared with the same materials without Au, which may have potential applications in biological detection and nanoreactors [34].

This notable enhancement phenomenon stems from a resonant excitation of surface Plasmon polarizations confined within a metallic nanostructure leading to a consequent enhancement in the induced dipole moment of the electronic transition responsible for the emission. Based on some studies, research on the fabrication of plasmonic nanomaterials and their high potential for various applications in photonics and surface-enhanced spectroscopy resulted in an increasing interest about the fundamental physics of the metal nanoparticles [35–39]. Moreover, many papers have been published regarding the effect of Ag metallic nanoparticles on the structure of annealed silica obtained by sol–gel method.

In this work, we have focused on an easy method to prepare the luminescent materials Y_2O_3 and $Y_2O_3:Eu^{3+}$ (5 mol% Eu^{3+}) using citrate precursors. Also, the effect of Ag nanoparticles on the spectroscopic and structural properties of the doped material was investigated.

* Corresponding author. Fax: +55 16 3633 2660.
E-mail addresses: jeffersonlferrari@gmail.com, ferrari@pg.ffclrp.usp.br (J.L. Ferrari).

0022-4596/$ - see front matter © 2010 Elsevier Inc. All rights reserved.
doi:10.1016/j.jssc.2010.07.010

2. Experimental procedure

As reported by Ferrari et al. [30] in previous work based on spectroscopic properties, the best concentration of Eu^{3+} in the Y_2O_3 host matrix prepared by citrate precursor is 5 mol%. Y_2O_3, Y_2O_3:Eu^{3+} (5 mol% Eu^{3+}) and Y_2O_3:Eu^{3+} (5 mol% Eu^{3+}) containing 1 mol% of Ag were prepared by citrate method [27–29]. Yttrium oxide (Aldrich 99.999%), europium oxide (Aldrich 99.999%) and silver nitrate (Acros Organic 99%) were used to obtain the respective nitrate solutions with concentration of metals of 9.95×10^{-3}, 1.3×10^{-2} and 0.01 mol L^{-1}, respectively, to obtain the stock solution. The volume of nitrate metal solutions and the amount of citric acid (Vetec, P.A.) (the number of moles of citric acid was 20 times that of the number of moles of metals) to prepare each material were added in the beaker and deionized water was added to complete 50 mL of final solution. Stoichiometric amounts of the reagents were used to obtain 1 g of Y_2O_3, Y_2O_3:Eu^{3+} (5 mol% Eu^{3+}) and Y_2O_3:Eu^{3+} (5 mol% Eu^{3+}) containing 1 mol% of Ag of final product. The amount of citric acid changes for each samples, because the amount of metals also changes. Then, ammonium hydroxide solution (0.01 mol L^{-1}) was added drop by drop to adjust the pH to 4 to facilitate the formation of homogeneous solution and to avoid possible metal hydrolysis reaction, and the solution was slowly evaporated upon 80 °C until the formation of a viscous resin. For the obtainment of the resin, the solutions were prepared in dark environment to avoid the reduction of silver by light. After that, the resins were fired in an oven at 800 °C for 4 h to give the three materials. The powder samples were characterized by X-ray diffractometry (XRD) using a Rigaku RINT 2000 (copper target, $\lambda=1.5406$ Å) at a scanning rate of 0.03°/2 s (15–70°, 2θ range). High resolution transmission electron microscopy (HRTEM) and energy-dispersive X-ray spectrometry (EDS) analyses were acquired using a Philips CM 200 transmission electron microscope in order to study the morphology, grain size and composition of the particles. HRTEM images were also used to determine an average particle size as well as the size distribution and to build the histograms. The nanoparticles were suspended in isopropyl alcohol and added onto copper grade to support the samples the during analyses. Photoluminescence (PL) spectroscopy measurements were carried out using a Fluorolog SPEX F212/Jobin-Yvon fluorescence spectrometer equipped with an R928 Hamamatsu photomultiplier. A 450 W ozone-free Xenon lamp was used as the excitation source equipped with a cooled Hamamatsu R928 photomultiplier with excitation and emission slits fixed at 0.3 and 0.5 mm, respectively. Emission spectra in the range between 575 and 700 nm of Y_2O_3:Eu^{3+} (5 mol% Eu^{3+}) and Y_2O_3:Eu^{3+} (5 mol% Eu^{3+}) containing 1 mol% of Ag were obtained at room temperature with excitation at 261 nm, in the region of the charge-transfer band related to the excitation of an electron from the oxygen 2*p* state to Eu^{3+} 4*f* state [32,40–42].

3. Results and discussion

Fig. 1 shows the XRD patterns of Y_2O_3, Y_2O_3:Eu^{3+} (5 mol% Eu^{3+}) and Y_2O_3:Eu^{3+} (5 mol% Eu^{3+}) containing 1 mol% of Ag prepared from citrate precursors. The cubic structure of Y_2O_3 appears as the main phase and is present in all the formed materials. Jung et al. [12] observed that the pure cubic phase of Y_2O_3 is obtained from spray pyrolysis in the temperature range from 800 to 1300 °C without transition to the monoclinic phase.

This crystalline system corresponds to a body-centered cubic structure with Ia_3 space group consistent with the JCPDS no. 43-1036 card [43]. It is well known that the Y^{3+} ions are accommodated in two different symmetries, i.e., the C_2 without inversion center and the S_6 with inversion center [26,44].

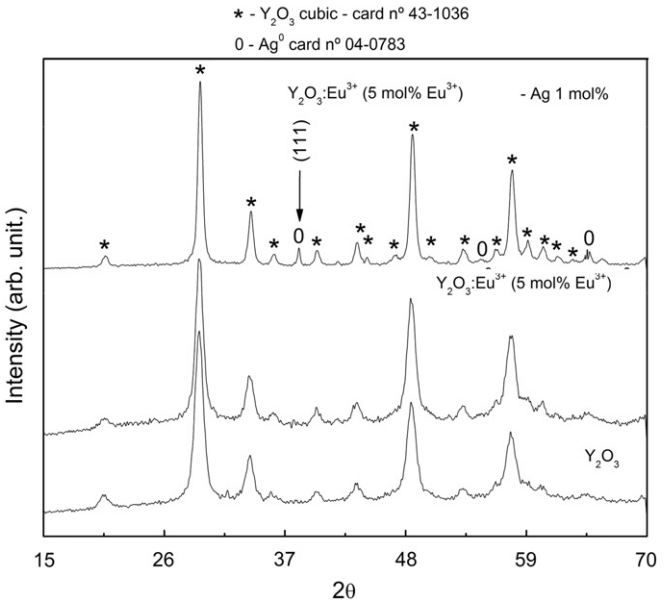

Fig. 1. X-ray diffraction patterns of Y_2O_3, Y_2O_3:Eu^{3+} (5 mol% Eu^{3+}) and Y_2O_3:Eu^{3+} (5 mol% Eu^{3+}) containing 1 mol% of Ag samples obtained by heat treating the resin prepared by citrate precursor at 800 °C for 4 h in static air atmosphere. The assignments of the indexed phases are also indicated (inset).

The Eu^{3+} ion might be replacing the Y^{3+} ions in the Y_2O_3 host lattice because no diffraction pattern characteristic of Eu_2O_3 phase is detected. This is an expected effect since the difference between the Y^{3+} and Eu^{3+} atomic radii is quite small (0.047 Å) [30,45]. Through careful examination of the powder XRD patterns of phosphors with Ag content, it can be observe the extra reflection peaks that are assigned to the metallic Ag phase, which are consistent with the JCPDS no. 04-0783 card [46]. The peak of Ag is localized around $2\theta=38.25°$ and assigned to the (1 1 1) plane. In addition, a comparison among the half-band widths of the diffraction peaks from the different samples (Fig. 1) suggests that the Ag nanoparticles lead to sharper peaks referent to the Y_2O_3 in the diffractograms, and this effect may be related to an increase of the system crystallinity. In accordance to Herd et al. [47] the addition of small amount of metals to some materials, the metal-induced crystallization effect occurs, contributing to increasing the crystallinity, or then, the formation of phases that are normally obtained at higher temperature. Using an XRD diffractogram, it was possible to estimate of the average nanocrystallite size by Scherrer's formula. The equation is described by the relation $t=0.89\lambda/B\cos\theta$, where t is an average nanocrystallite size, $\lambda_{\AA}$ the X-ray wavelength, B the full width half-maximum (FWHM) and θ_{rad} the position of the peak used in calculus. The estimations were realized based on the reflection peaks localized near $2\Theta=29.28°$ assigned to the (2 2 2) main plane present in the diffractograms and the average nanocrystallite sizes for Y_2O_3, Y_2O_3:Eu^{3+} (5 mol% Eu^{3+}) and for Y_2O_3:Eu^{3+} (5 mol% Eu^{3+}) in the sample containing 1 mol% of Ag, were 9.6, 9.6 and 16.9 nm, respectively. According to Taxak et al. [22], the Y_2O_3:Eu^{3+} nanoparticles obtained via tartaric acid sol–gel method, depicted nanocrystallite with size around 20 nm for materials annealed at 500 °C and 45 nm for material annealed at 800 °C/3 h. Recently, Wang et al. [48] reported the obtaining of Y_2O_3:Eu^{3+} by homogeneous precipitation, and observed the formation of nanocrystallite size around 41 and 30 nm dependeing on the amount of europium and also the pH chosen in the reaction. As we can see, the method reported in this work contributes to obtaining Y_2O_3:Eu^{3+} material with smaller nanocrystallites size in comparison with other works reported in the literature.

TEM images of the materials annealed at 800 °C for 4 h in air are depicted in Fig. 2. Fig. 2(a) shows Y_2O_3:Eu^{3+} (5 mol% Eu^{3+}) with an average particle size of 12 nm. EDS analysis evidences the presence of a pure material composed only by yttrium, europium and oxygen. The assigned energy peaks are in accordance with those reported by Yongqing et al. [14].

TEM and EDS analyses of the sample containing 1 mol% of Ag present in two different areas with different particle sizes and are indentified as areas A and B (Fig. 2b). Area A is formed by nanoparticles composed basically of Y_2O_3:Eu^{3+} with an average size of 25 nm and area B by nanoparticle with size of about 9 nm. The HRTEM images and EDS spectra of the nanoparticles depicted in area B of Fig. 2(b) were recorded and are shown in Fig. 2(c). It is possible to observe that the nanoparticles are composed by Ag nanoparticles with an average size of about 9 nm. The copper lines detected in all the EDS spectra are related to the copper grade used to support samples for the HRTEM analysis. The statistical histograms of average nanoparticle size are shown in Fig. 3. Fig. 3(a) shows the histogram of the Y_2O_3:Eu^{3+} (5 mol% Eu^{3+}) nanoparticles in the absence of Ag while Fig. 3(b) shows the histogram of the Y_2O_3:Eu^{3+} (5 mol% Eu^{3+}) nanoparticles (area A) and the Ag nanoparticles (area B). The histograms show that the Ag nanoparticles promote an increase of the Y_2O_3:Eu^{3+} (5 mol% Eu^{3+}) particle size compared with the material obtained in the absence of Ag nanoparticles. In general, the particle size of the Y_2O_3:Eu^{3+} obtained by other researchers is very similar. Camenzind et al. [17] observed that the particle size of Y_2O_3:Eu^{3+} also containing 5 mol% of Eu^{3+}obtained by one-step flame spray pyrolysis depicts the size distribution between 10 and 25 nm that is dependent directly on the flame conditions. Dhanaraj et al. [23] prepared Y_2O_3:Eu^{3+} by the gel–polymers pyrolysis process and obtained materials with nanoparticles between 10 and 20 m. Schmechel et al. [6] also reported the formation of Y_2O_3:Eu^{3+} nanoparticles around 10 nm obtained from chemical vapour synthesis with great optical properties.

The diffuse reflectances were recorded for samples with and without Ag nanoparticles and the spectra obtained are depicted (Fig. 4(a)). By analysing the reflectance spectra profile, it is possible to verify that the investigated materials exhibit considerable differences. Firstly, Y_2O_3:Eu^{3+} (5 mol% Eu^{3+}) containing 1 mol% of Ag shows a reflectance edge in a region with higher energy in comparison with the sample without Ag nanoparticle. Secondly, in the spectrum of the sample containing Ag nanoparticles, an absorption band around 400 nm is observed and can be assigned to the plasmon surface effect, which is usually displayed by metallic nanoparticles [49,50]. On the other hand, in the Y_2O_3:Eu^{3+} (5 mol% Eu^{3+}) spectrum this band is absent and a band edge is observed in lower energy. The band assigned to the plasmon effect, helps us verify the Ag nanoparticles that are present, and the results obtained by XRD, HRTEM and EDS also contribute to confirm with this observation. The position of the band localized in higher energy observed in the reflectance spectrum may be associated to the presence of Ag nanoparticles, which are responsible for eliminating the possible defects present on the surface of Y_2O_3:Eu^{3+} material, due to the metal-induced crystallization effect. Consequently, the elimination of defects can lead to a more transparent Y_2O_3:Eu^{3+} material in the visible range containing Ag nanoparticles in comparison to the material without Ag nanoparticles. The bandgap values of the compounds were determined by using

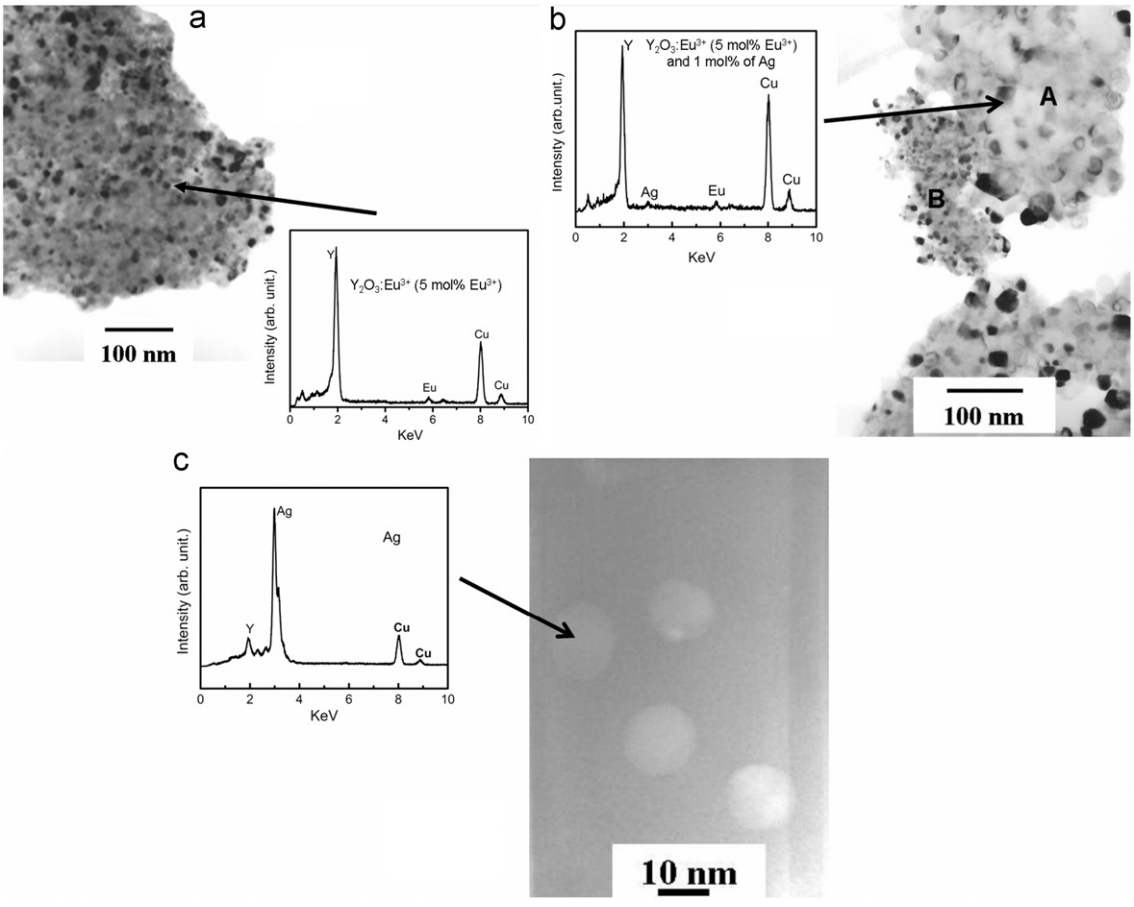

Fig. 2. TEM images and EDS analysis of (a) Y_2O_3:Eu^{3+} (5 mol% Eu^{3+}), (b) Y_2O_3:Eu^{3+} (5 mol% Eu^{3+}) containing 1 mol% of Ag and (c) HRTEM image and EDS analysis of the Ag nanoparticles.

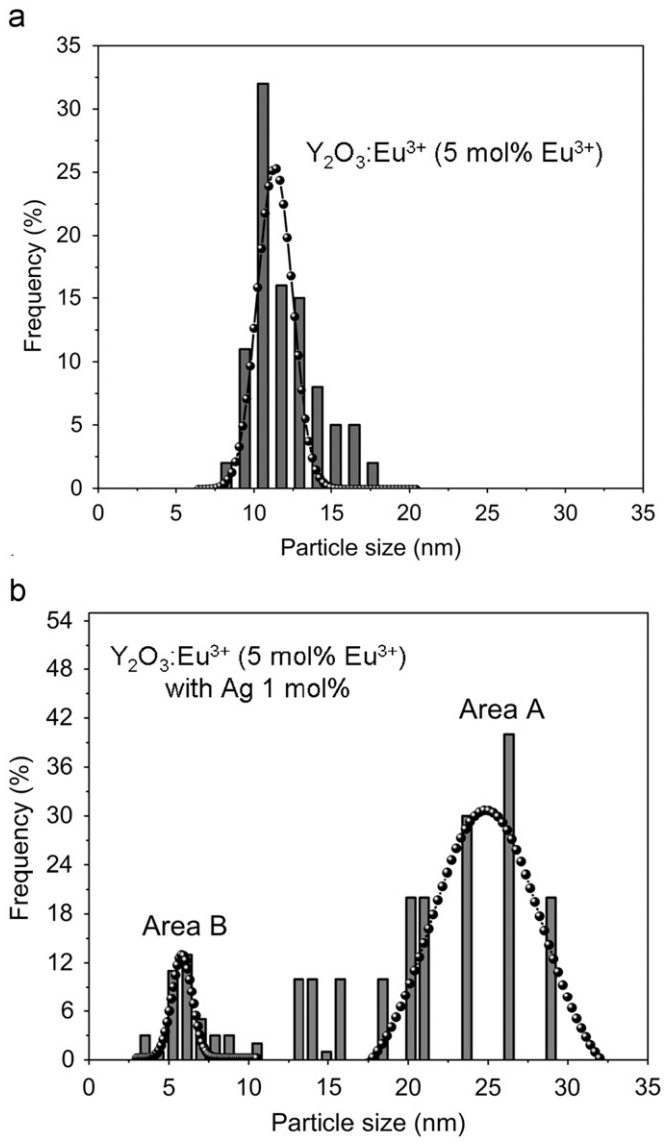

Fig. 3. Representative particle size histograms of (a) Y_2O_3:Eu^{3+} (5 mol% Eu^{3+}) and (b) Y_2O_3:Eu^{3+} (5 mol% Eu^{3+}) containing 1 mol% of Ag (area A=Y_2O_3:Eu^{3+} (5 mol% Eu^{3+}) and area B=Ag nanoparticles) obtained by heat treating the resin prepared by citrate precursor at 800 °C for 4 h in static air atmosphere.

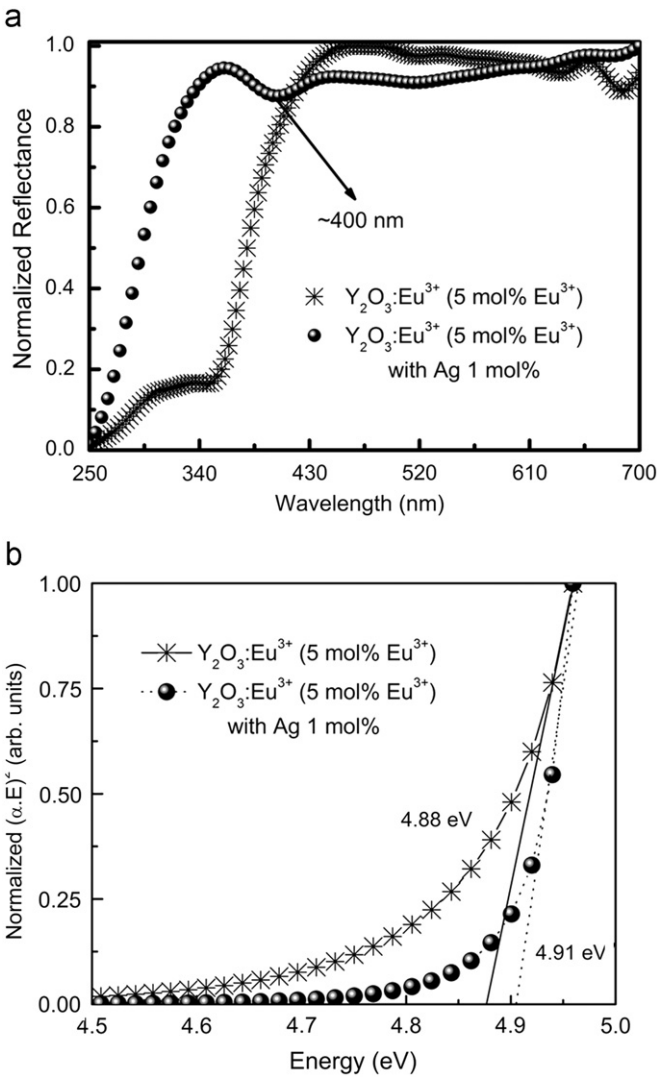

Fig. 4. (a) Diffuse reflectance spectra of Y_2O_3:Eu^{3+} (5 mol% Eu^{3+}) and Y_2O_3:Eu^{3+} (5 mol% Eu^{3+}) containing 1 mol% of Ag nanoparticles and (b) calculated bandgap of Y_2O_3:Eu^{3+} (5 mol% Eu^{3+}) and Y_2O_3:Eu^{3+} (5 mol% Eu^{3+}) containing 1 mol% of Ag nanoparticles obtained by heat treating the resin prepared by citrate precursor at 800 °C for 4 h in static air atmosphere.

the Kubelka–Munk model with the Tauc, considering an indirect bandgap for Y_2O_3 host matrix [50]. The determined bandgap depicted in Fig. 4(b) leads to the same conclusion, that is, if the compound containing 1% of Ag nanoparticles possess a higher crystallinity than Y_2O_3:Eu^{3+} (5 mol% Eu^{3+}) then one would expect a higher bandgap for it.

Fig. 5 shows the emission spectra. The emission observed in the 575–700 nm range is ascribed to the well-known Eu^{3+} $^5D_0 \rightarrow {}^7F_J$ (J=0, 1, 2, 3 and 4) transitions. The maximum intensity at 612 nm is assigned to the hypersensitive $^5D_0 \rightarrow {}^7F_2$ transition due to the forced electric dipole mechanism. All the other emission peaks at ~580 ($^5D_0 \rightarrow {}^7F_0$–$C_2$), 582 ($^5D_0 \rightarrow {}^7F_1$–$S_6$) and at 587, 593 and 599 nm ($^5D_0 \rightarrow {}^7F_1$) were assigned and are shown in Fig. 5(a). In the cubic Y_2O_3 there are two crystallographic sites, one with C_2 symmetry and the other with S_6 symmetry. Therefore, it can be concluded that the Eu^{3+} ions replace the Y^{3+} ions and occupy both the C_2 and S_6 symmetries because the emissions assigned to such symmetries were observed (Fig. 5(b)). As discussed in the XRD results, the Ag nanoparticles may be affecting the crystallinity of the system and consequently the neighbourhood around the Eu^{3+} ions. This effect can be verified by the shift observed in the emission spectra assigned to $^5D_0 \rightarrow {}^7F_0$ (C_2), $^5D_0 \rightarrow {}^7F_1$ (S_6) and $^5D_0 \rightarrow {}^7F_1$ (Fig. 5(b)). On the basis of the Judd–Ofelt theory [40,51,52], the $^5D_0 \rightarrow {}^7F_0$ and $^5D_0 \rightarrow {}^7F_1$ transitions originate from electric and magnetic dipoles, respectively. The electric dipole transition is allowed only when Eu^{3+} occupies a site without an inversion center and is sensitive to the local symmetry. Thus the shift observed in the spectrum of the sample containing Ag is due to a microstructural change in the host lattice, formed by the presence of Ag nanoparticles.

Luminescence efficiency for the materials reported in the current work is unknown and still in progress. However, the phosphor containing Ag nanoparticles shows higher intensity luminescence, and displays around 34% more relative intensity than the sample without Ag nanoparticles. This observation is very important to certify that the Ag nanoparticles contribute to the optical properties of the material obtained from citrate precursors. The plasmon effect observed on the Ag nanoparticles may contribute to an increase of the relative luminescence intensity of Eu^{3+}-doped Y_2O_3 host lattice (5 mol% Eu^{3+}) as well

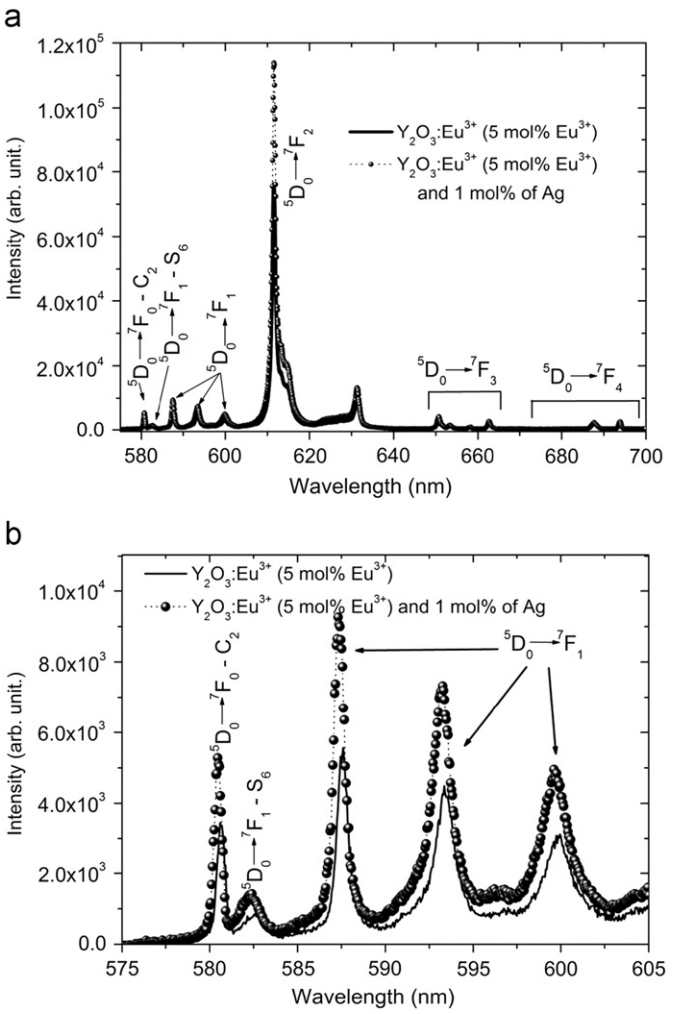

Fig. 5. (a) Photoluminescence emission spectra of Y_2O_3:Eu^{3+} (5 mol% Eu^{3+}) and Y_2O_3:Eu^{3+} (5 mol% Eu^{3+}) containing 1 mol% of Ag nanoparticles in the region between 575 and 700 nm and (b) photoluminescence emission spectra of Y_2O_3:Eu^{3+} (5 mol% Eu^{3+}) and Y_2O_3:Eu^{3+} (5 mol% Eu^{3+}) containing 1 mol% of Ag nanoparticles in the region of the $^5D_0 \rightarrow {}^7F_0$ and $^5D_0 \rightarrow {}^7F_1$ emissions (C_2 and S_6 symmetries, respectively), obtained by heat treating the resin prepared by citrate precursor at 800 °C for 4 h in static air atmosphere.

as an improvement of the crystallinity. The addition of Ag nanoparticle may also favor the electron transition of the Eu^{3+}, which could enhance the emission intensity. In accordance to Jung et al. [12], the increase of crystallinity due to the post-treatment in temperature between 800 and 1330 °C, is responsible for the enhancement of the photoluminescence intensity of the same material obtained by spray pyrolysis. The authors also observed that the crystallinity of the materials is more significant than the surface area and also the enlargement of the crystallite size to enhance the luminescent intensity of Y_2O_3:Eu^{3+} obtained by the spray pyrolysis route.

Therefore, in this work we have observed that the Ag nanoparticles affect the crystallinity of the system and the study of the emission of Y_2O_3:Eu^{3+} (5 mol% Eu^{3+}) with the presence of different amounts of Ag nanoparticles is in development.

4. Conclusions

The citrate method used in this work demonstrated to be a suitable route to prepare Y_2O_3:Eu^{3+} (5 mol% Eu^{3+}) containing 1 mol% of Ag nanoparticles. This route can also be considered as feasible for the synthesis of crystalline materials. The plasmon surface effect was also observed for Y_2O_3:Eu^{3+} (5 mol% Eu^{3+}) containing Ag nanoparticles, thus confirming the presence of metal nanoparticles together with the XRD and HRTEM analyses. The presence of the Ag nanoparticles in the Y_2O_3 host lattice might promote a decrease of the defects possibly present on the particle surface, which can affect the Eu^{3+} neighbourhood. The metal-induced crystallization effect was observed in this work, and can be the main effect to contribute for the luminescence enhancement of Y_2O_3:Eu^{3+} (5 mol% Eu^{3+}). However, a systematic study about the plasmon effect or host crystallinity on the enhancement of luminescence as a function of different amounts of Ag is still in progress.

Acknowledgments

The authors acknowledge the funding agencies FAPESP and CNPq for the financial support. J.L. Ferrari thanks FAPESP for the scholarship.

References

[1] G. Blasse, B.C. Grabmaier, in: Luminescent Materials, Springer, Berlin, Germany, 1994.
[2] M. Jia, J. Zhang, S. Lu, S. Sun, Y. Luo, X. Ren, H. Song, X. Wang, Chem. Phys. Lett. 384 (2004) 193.
[3] S. Ray, P. Pramanik, A. Singha, A. Roy, J. Appl. Phys. 97 (2005) 094312-1.
[4] J.W. Wang, Y.M. Chang, H.C. Chang, S.H. Lin, L.C. Huang, X.L. Kong, M.W. Kang, Chem. Phys. Lett. 405 (2005) 314.
[5] J. Wan, Z. Wang, X. Chen, L. Mu, Y. Qian, J. Cryst. Growth 284 (2005) 538.
[6] R. Schmechel, M. Kennedy, H. Von Seggern, H. Winkler, M. Kolbe, R.A. Fischer, L. Xaomao, A. Benker, M. Winterer, H. Hahn, J. Appl. Phys. 89 (2001) 1679.
[7] H.W. Song, B.J. Chen, H.S. Peng, J.S. Zhang, Appl. Phys. Lett. 81 (2002) 1776.
[8] X.M. Li, A. Benker, M. Winterer, H. Hahn, J. Appl. Phys. 89 (2001) 1679.
[9] G.Y. Hong, K. Yoo, S.J. Moon, J.S. Yoo, J. Electrochem. Soc. 150 (2003) H67.
[10] G. Wakefield, E. Holland, P.J. Dobson, J.L. Hutchison, Adv. Mater. 20 (2001) 1557.
[11] H. Peng, H. Song, B. Chen, S. Lu, S. Huang, Chem. Phys. Lett. 370 (2003) 485.
[12] K.Y. Jung, C.H. Lee, Y.C. Kang, Mater. Lett. 59 (2005) 2451.
[13] R. Debnath, A. Nayak, A. Ghosh, Chem. Phys. Lett. 444 (2007) 324.
[14] Z. Yongqing, Y. Zihua, D. Shiwen, Q. Mande, Z. Jian, Mater. Lett. 57 (2003) 2901.
[15] N. Rakov, W. Lozano, G.S. Maciel, C.B. Araújo, Chem. Phys. Lett. 428 (2006) 134.
[16] H. Song, B. Chen, B. Sun, J. Zhang, S. Lu, Chem. Phys. Lett. 372 (2003) 368.
[17] A. Camenzind, R. Strobel, S.E. Pratsinis, Chem. Phys. Lett. 415 (2005) 193.
[18] L.S. Wang, Y.H. Zhou, Z.W. Quan, J. Lin, Mater. Lett. 59 (2005) 1130.
[19] M.R. Davolos, S. Feliciano, A.M. Pires, R.F.C. Marques, M.J. Jafelicci Jr, J. Solid State Chem. 171 (2003) 268.
[20] Y. Sun, L. Qi, M. Lee, B.I. Lee, W.D. Samuels, G.J. Exarhos, J. Lumin. 109 (2004) 85.
[21] O.A. Graeve, J.O. Corral, Opt. Mater. 29 (2003) 24.
[22] V.B. Taxak, S.P. Khatkar, S.D. Han, R. Kumar, M. Kumar, J. Alloys Compd. 469 (2008) 224.
[23] J. Dhanaraj, R. Jagannathan, T.R.N. Kutty, C.H. Lu, J. Phys. Chem. B 105 (2001) 11098.
[24] M.K. Chong, K. Pita, C.H. Cam, Mater. Chem. Phys. 100 (2006) 329.
[25] A. Pandev, A. Pandev, M.K. Roy, H.C. Verma, Mater. Chem. Phys. 96 (2006) 466.
[26] Q. Pang, J. Shi, Y. Liu, D. Xing, M. Gong, N. Xu, Mater. Sci. Eng. B 103 (2003) 57.
[27] H. Guo, W.P. Zhang, N. Dong, L.R. Lou, M. Yin, O. Tillement, J. Mugnier, E. Bernstein, P.F. Brevet, J. Rare Earths 23 (2005) 600.
[28] J. Zhang, Z. Zhang, Z. Tang, Y. Lin, Z. Zheng, J. Mater. Proc. Technol. 121 (2002) 265.
[29] J. Zhang, Z. Tang, Z. Zhang, W. Fu, J. Wang, Y. Lin, Mater. Sci. Eng. A 334 (2002) 246.
[30] J.L. Ferrari, A.M. Pires, M.R. Davolos, Mater. Chem. Phys. 113 (2009) 587.
[31] Y. Xua, P. Lu, G. Huang, C. Zeng, Mater. Chem. Phys. 95 (2006) 62.
[32] Z. Liu, H. Song, R. Qin, G. Pan, X. Bai, Solid State Commun. 137 (2006) 199.
[33] H. Nabica, S. Deki, J. Phys. Rev. B 107 (2003) 9161.
[34] Y.L. Min, Y. Wan, S.H. Yu, Solid State Sci. 11 (2009) 96.
[35] P.V. Drachev, E.N. Khalullin, W. Kim, F. Alzoubi, S.G. Rautian, V.P. Safonov, R.L. Armstrong, V.M. Shalaev, Phys. Rev. B 69 (2004) 035318.
[36] O.L. Malta, M.A. Couto dos Santos, L.C. Thompson, N.K. Ito, J. Lumin. 69 (1996) 7.
[36] T. Hayakawa, S.T. Selvan, M. Nogami, Appl. Phys. Lett. 74 (1999) 1513.
[38] O.L. Malta, M.A. Couto dos Santos, Chem. Phys. Lett. 174 (1990) 13.
[39] M.A. Couto dos Santos, O.L. Malta, G.F. Sá, J. Alloys Compd. 180 (1992) 215.

[40] J.Y. Zhang, Z.T. Zhang, Z.L. Tang, Y.H. Lin, Z.S. Zheng, J. Mater. Process. Technol. 121 (2002) 265.
[41] Y.Q. Zhai, Z.H. Yao, S.W. Ding, M.D. Qiu, J. Zhai, Mater. Lett. 57 (2003) 2901.
[42] Y. Nakanishi, H. Wada, H. Kominami, M. Kottaisamy, T. Aoki, Y. Hatanaka, J. Electrochem. Soc. 146 (11) (1999) 4320.
[43] Joint Committee on Powder Diffraction Standards, Diffraction Data File, no. 43-1036—JCPDS International Center for Diffraction Data, Pennsylvania, 1991.
[44] J.C. Park, H.K. Moon, D.K. Kim, S.H. Byeon, B.C. Kim, K.S. Suh, Appl. Phys. Lett. 77 (2000) 2162.
[45] J.A. Huhhey, E.A. Keiter, R.L. Keiter, in: Inorganic Chemistry, HarperCollins, New York, 1993.
[46] Joint Committee on Powder Diffraction Standards, Diffraction Data File, no. 04-0783—JCPDS International Center for Diffraction Data, Pennsylvania, 1991.
[47] S.R. Herd, P Chaudhari, M.H. Brodsky, J. Non-Cryst. Solids 7 (1972) 309.
[48] C.N. Wang, Y. Li, W.P. Zhang, M. Yin, Spectrochim. Acta Part A 75 (2010) 8.
[49] P.V. Kamat, M. Flumiani, G.V. Hartland, J. Phys. Chem. B 102 (1998) 3123.
[50] E.M. Patterson, C.E. Shelden, B.H. Stockton, Appl. Opt. 16 (1977) 729.
[51] B. Judd, Phys. Rev. 127 (1962) 750.
[52] G. Ofelt, J. Chem. Phys. 37 (1962) 511.